American Mineralogist, Volume 87, pages 1377–1383, 2002

Fluorite particles inducing butterfly aggregates of incipient microperthite in alkali feldspar from a syenite, the Patagonian Andes, southern Chile

SATOSHI NAKANO,[1,*] JUNJI AKAI,[2] AND ASAHIKO SUGAKI[3]

[1]Department of Natural Science, Faculty of Education, Shiga University, Otsu 520-0862, Japan
[2]Department of Geological Sciences, Faculty of Science, Niigata University, Niigata 950-2181, Japan
[3]Kadan 4-30-503, Aoba, Sendai 980-0966, Japan

ABSTRACT

Alkali feldspar grains found in a syenite from the Patagonian Andes, southern Chile, have bulk compositions of about $Or_{40}Ab_{59}An_{0.5}$, and consist of two parts when viewed under an optical microscope: a clear part and a turbid part. Grain interiors are mixtures of the two parts, whereas the rims are mainly turbid. The microscopically clear part, which is almost free of micropores, is cryptoperthitic, whereas the turbid part is microperthitic. The microperthite is of the patch type, and the turbidity is due to abundant micropores that are polygonal and generally less than 1 μm in diameter. The patch microperthite has been formed by coarsening of primary cryptoperthite by hydrothermal reactions. An incipient stage of the microperthite formation is recorded as the segregation of the Or-rich feldspar with diagonal elongation and Ab-rich feldspar into aggregates that have a "butterfly" shape. Each butterfly aggregate of microperthite is generally less than 10 μm in length. The centers of the butterfly aggregates are usually occupied by round fluorite particles about 1 μm in diameter, which were identified by EPMA and TEM analyses. The fluorite particles may have been formed at the fluid stage. The microperthite formation may have started as butterfly aggregates along the interfaces with the fluorite particles at the hydrothermal stage. The butterfly aggregates have changed to patch microperthite with further coarsening. The timing and process of the formation of the fluorite particles are important in relation to the evolution of feldspar microtextures, and the behavior of fluorine in alkaline igneous rocks.

INTRODUCTION

The model that the coarsening of cryptoperthite to microperthite is promoted by the presence of water as a catalyst was developed from studies of alkali feldspars in the Klokken syenite, southwest Greenland (Parsons 1968; Parsons and Brown 1984; Smith and Brown 1988; etc.). The model of these authors involves subsolidus reactions to form microtextures expected in ternary and alkali feldspars accompanying cooling of syenitic intrusions from magmatic to hydrothermal stages. However, many problems remain in understanding the details of such reactions, especially regarding the coarsening of cryptoperthitic intergrowths. New information on the textural and compositional variations of such subsolidus feldspar reactions has been obtained from studies of alkali feldspars in other syenite intrusions (Waldron and Parsons 1994; Nakano et al. 1997; Nakano 1998). In addition, the mechanism of incipient coarsening of microperthite has been discussed for the formation of vein-like microperthite along grain boundaries or cleavages, which has been named "pleat" (Lee et al. 1997; Brown et al. 1997).

Alkali feldspar grains in a syenite sample from the Patagonian Andes, southern Chile, microscopically consist of two parts: one that is clear and another that is turbid. This textural feature is not unlike that reported previously in alkali feldspars from other syenites (Parsons 1968; Lalonde and Martin 1983; Parsons and Brown 1984; Smith and Brown 1988; Waldron and Parsons 1994; Nakano et al. 1997; Nakano 1998; etc.). An incipient type of microperthite, which comprises an aggregate of Or-rich feldspar showing diagonal elongation and Ab-rich feldspar, forms a characteristic butterfly shape on (001). The centers of each butterfly aggregate are occupied by fluorite particles. This is a new occurrence of fluorite in feldspar. Microperthite formation seems to have started along the interfaces with the particles. These observations suggest that F may play an important role in the textural evolution of alkali feldspar in alkaline igneous rocks. In this paper, we describe the occurrence of the fluorite particles and butterfly aggregates in the feldspar, and discuss their formation processes from the viewpoint of subsolidus reactions forming microperthite in alkali feldspar under plutonic conditions.

GEOLOGIC SETTING AND SAMPLE DESCRIPTION

The Cerro Balmaceda pluton (51°25'S, 73°10'W) is one of several Miocene intrusions and subvolcanic rocks that crop out in a north-south belt in the foothills of the southern Andes in Chile (Michael 1985, 1991; Fig. 1). The plutons crop out in the transitional zone between the Mesozoic-Cenozoic Patagonian batholith in its western side and Cenozoic plateau lavas in its eastern side. The emplacement of the plutons in this distinctive position during the Miocene may be related to subduction of the Chile Ridge at these latitudes in Miocene-Recent times (Cande and Leslie 1986; Michael 1983, 1991). The Quaternary calc-alkaline volcanoes are distributed close to and in par-

* E-mail: nakano@sue.shiga-u.ac.jp

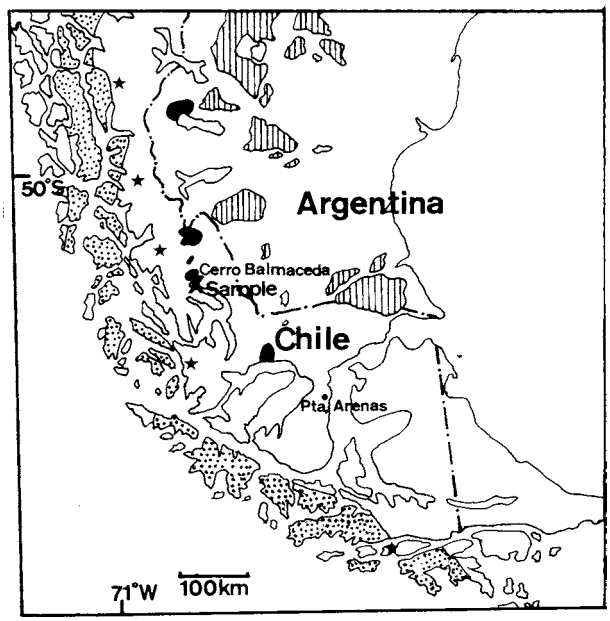

FIGURE 1. Regional geological map around Cerro Balmaceda and sampling locality [after Michael (1991)]. Black areas show Miocen pluton and subvolcanic rocks.

allel with these plutons in their western side. The details of the Cerro Balmaceda pluton have not been reported anywhere as far as the authors know, and Michael (1991) noted only that it is undated and alkaline. Calc-alkaline plutons of Cerro Donoso and Cordillera del Paine in the same zone are situated just north of the Cerro Balmaceda pluton, and the Cordillera Pinto shoshonite complex is located about 200 km to the south. Of these intrusions, only the Cordillera del Paine pluton was investigated in detail (Michael 1983, 1991).

The rock sample examined in this study is from a miarolitic facies of a fine-grained syenite at the foothill of Cerro Balmaceda. The details of this occurrence are unknown, because of the limited time spent at the sampling place, which is a small harbor at the eastern foothill of Cerro Balmaceda. The sample contains tabular grains of alkali feldspar, 1–2 cm in length and ~8 mm in width. When examined with the naked eye, the feldspars show color zoning in which a pale pink, opaque rim encloses a gray, translucent interior and penetrates into it.

TEXTURES AND COMPOSITIONS OF FELDSPAR

Perthitic textures

Alkali feldspar grains show rim-interior color zoning, as noted above. The boundaries between interiors and rims are not so distinct microscopically or texturally as seen with the naked eye (Fig. 2). Both the rims and the interiors consist of two parts when viewed under a microscope: one is clear, and the other is turbid.

The clear part is cryptoperthitic, as shown by the lamellar textures observed with a transmission electron microscope (TEM, Fig. 3). Braid cryptoperthite has not yet been observed, which is different from the textures presented by Brown and

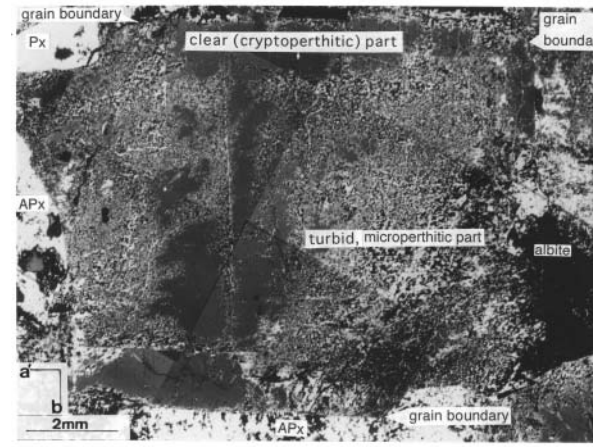

FIGURE 2. BSE image showing a view of an entire alkali feldspar grain (joined photographs). Inclined (001) section. Px = pyroxene, APx = altered pyroxene.

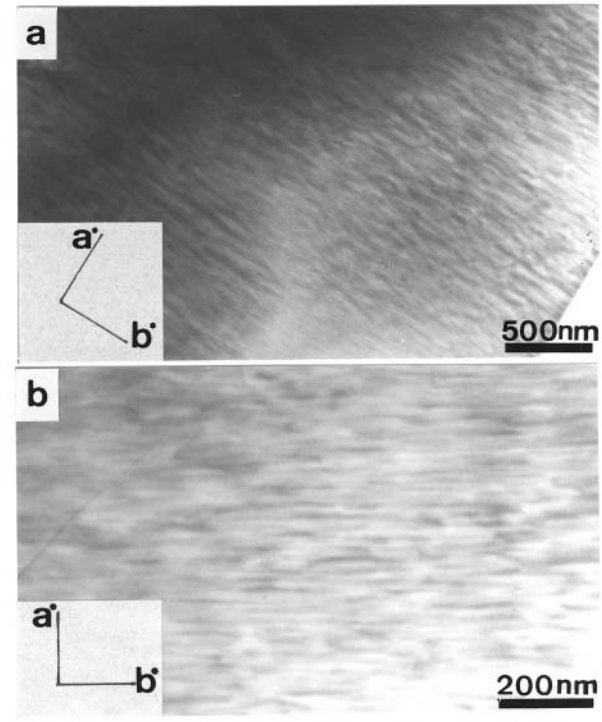

FIGURE 3. TEM photomicrographs showing cryptoperthitic textures (**a**, **b**).

Parsons (1988). Observations using back-scattered electron (BSE) images revealed the presence of numerous small aggregates of Or- and Ab-rich feldspars in the clear part of the interiors (Fig. 4a), which appear only as faint, spike-like defects or cracks under the highest-power optical microscope examination. On (001) sections, the two-feldspar aggregates clearly form a butterfly shape (Fig. 4c).

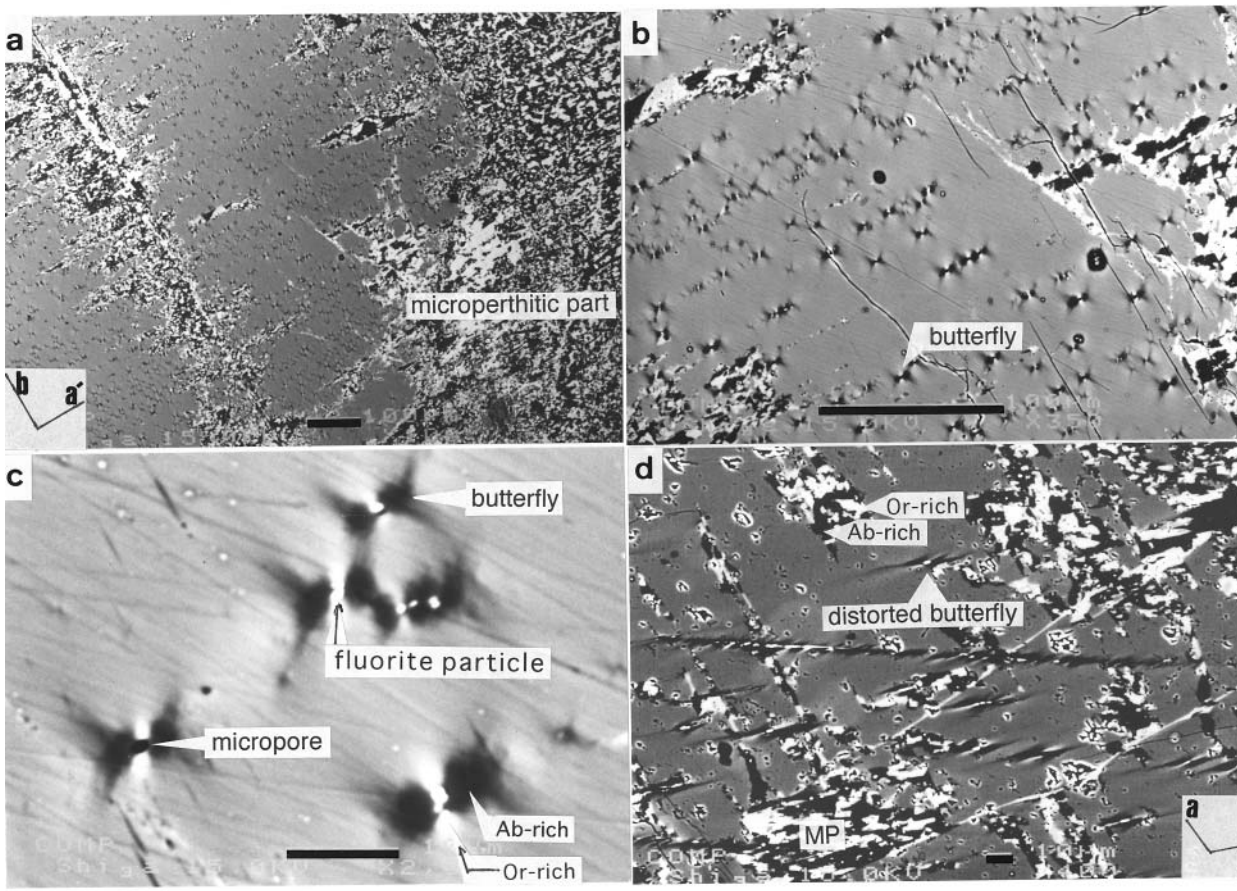

FIGURE 4. BSE images showing feldspar microtextures. Three photographs (**a**–**c**) show part of the feldspar grain shown in Figure 1. Parts **a**, **b**, and **c** are inclined (001) sections, and in the same orientation. Part **d** is a (010) section. Scales in **a** and **b** are 100 μm, and those in **c** and **d** are 10 μm. MP = patch microperthite.

This butterfly shape results from the aggregation of each of two Or-rich and Ab-rich feldspars contacting each other and having diffuse boundaries with the surrounding clear part (Fig. 5). In general, the Ab-rich feldspars are elongated approximately along the $(\bar{6}61)$ and $(\bar{6}01)$ traces. The Or-rich feldspars are elongated approximately along the $(\bar{6}01)$ trace. On (010) sections, the butterfly shape is distorted (Fig. 4d). In this paper, this two-feldspar microtexture is newly named "butterfly aggregate of microperthite," or "butterfly aggregate." Each butterfly aggregate is generally less than 10 μm in length. A linear distribution of butterflies is commonly observed along the trace of (010) on (001) sections (Figs. 4a, 4b), although it is not so clear on (010) sections (along the **a**-axis direction). The coalescence of several butterflies has been observed, with a resultant vein-like appearance, usually on (010) sections (Fig. 4d).

The turbid part consists of patch-type microperthite (Figs. 2 and 4), and is similar to that of the Japanese syenite feldspars in mosaic appearance (Nakano et al. 1997; Nakano 1998). It is noteworthy that the boundaries of constituent phases are often along the **a**-axis direction on (001) sections and along the $(\bar{6}01)$ trace on (010) sections. The coarseness and size of the patch microperthite vary from place to place. Small areas of the patch microperthite are observed adjacent to butterfly aggregates (Figs. 4c, 4d). The turbid, microperthitic part is characterized by abundant micropores as reported elsewhere by other investigators (Worden et al. 1990; Walker et al. 1995). The shape of the pores is polygonal rather than round. The micropores are around 1 μm in diameter on BSE and secondary-electron images (SEI), but are more variable on a TEM scale.

Compositional features

The compositions of the microscopically clear part of the intergrowths generally lie in the range between $Or_{31}Ab_{68}$ and $Or_{47}Ab_{52}$ with low An contents (0–1.4 mol%), although more Or-rich compositions may be encountered. Compositions richer in An commonly occur in the interiors, especially in the cores, which have an average composition of about $Or_{40}Ab_{59}An_1$. The feldspar compositions of the patch microperthite are close to the end-members. The Or-rich feldspar has compositions in the range $Or_{92-96}Ab_{7.7-4.5}An_{0-0.1}$, and the Ab-rich feldspar compositions are $Or_{3.8-1.4}Ab_{96-98}An_{0.2-1.5}$. The representative chemical com-

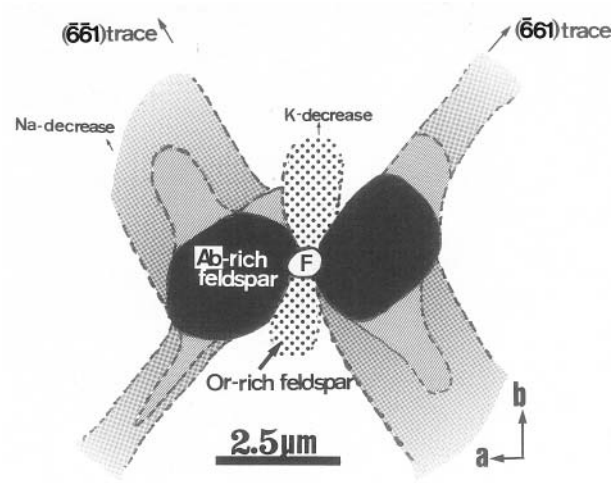

FIGURE 5. Schematic drawing of a butterfly aggregate from BSE observations on (001) sections. All the boundaries are conveniently lined except for the outline of a fluorite particle, because the compositional variations seem to be gradual and diffuse on BSE images. The elongation of Ab-rich feldspars nearly along the ($\bar{6}61$) and ($6\bar{6}1$) traces is characteristic.

TABLE 1. Representative chemical compositions of several types of feldspars in syenite from southern Chile

	Clear part		Turbid and microperthitic part			
	interior	rim	interior		rim	
			Or-rich	Ab-rich	Or-rich	Ab-rich
SiO_2	66.91	66.67	65.76	67.17	63.93	67.58
Al_2O_3	19.59	19.06	18.99	20.23	18.57	19.58
FeO	0.28	0.44	0.06	0.05	0.09	0.19
CaO	0.16	0.01	0.00	0.09	0.00	0.01
Na_2O	7.21	7.18	0.54	11.33	1.36	11.56
K_2O	6.90	6.66	15.95	0.16	16.27	0.49
BaO	0.00	0.00	0.08	0.00	n.d.	0.00
Total (wt%)	101.05	100.02	101.38	99.03	100.22	99.41
Formula proportions based on eight O atoms						
Si	2.970	2.986	2.991	2.963	2.981	2.979
Al	1.025	1.006	1.018	1.052	1.021	1.018
Fe	0.011	0.017	0.002	0.002	0.004	0.007
Ca	0.008	0.004	0.000	0.004	0.000	0.000
Na	0.621	0.623	0.047	0.969	0.041	0.988
K	0.391	0.381	0.926	0.009	0.968	0.028
Ba	0.000	0.000	0.001	0.000	n.d.	0.000
Total	5.026	5.017	4.985	4.999	5.015	5.020
End-member proportions in mol%						
An	0.8	0.4	0.0	0.4	0.0	0.0
Ab	60.9	62.1	4.8	98.7	4.1	97.2
Or	38.3	37.8	95.2	0.9	95.9	2.8

position of each feldspar mentioned above are shown in Table 1.

The compositional difference between the two types of clear feldspar (with and without butterfly aggregates), which were checked by broad-beam analyses using a 50 μm spot size (local bulk compositions), is not clear. The compositions of both parts are somewhat variable, around Or_{40} Ab_{60}, and their An contents also vary from place to place. The local bulk compositions of the turbid, microperthitic part vary to some extent in places, corresponding to textural differences depending on which feldspar (Or-rich or Ab-rich) is dominant. The average composition of the turbid part is nearly the same ($Or_{40}Ab_{60}$) as the representative composition of the clear part, but the turbid, microperthitic part generally contains negligible Ca. The bulk chemical composition, obtained by averaging the local bulk compositions, is $Or_{40}Ab_{59}An_{0.5}$.

FLUORITE IN BUTTERFLY AGGREGATES

There is a small particle in the center of each butterfly, whose nature was clarified by BSE observations. On (001) and (010) sections, the particles are round in shape, and vary from spherical to ellipsoidal. These particles were confirmed to be fluorite as follows. The X-ray maps of fourteen elements (K, Na, Ca, Al, Si, O, Ba, Fe, F, Cl, P, S, Mn, and Cu) show that only two elements, Ca and F, usually occur, and that other elements (including Si, Al, and O) are not present (Fig. 6).

The same particle was found by careful TEM observations (Fig. 7). EDS analyses with the TEM also show that the particle consists only of Ca and F. The measured *d*-spacing of its (110) plane obtained from TEM diffraction patterns coincides with that of fluorite. Round micropores are observed in some centers of the butterflies instead of particles. These micropores may result from removal of the fluorite particles during thin-section preparation. These particles and micropores are about 1 μm in diameter (Fig. 4c).

The linear (not zonal) distribution of particles is commonly observed along the trace of (010) on (001) sections (Figs. 4a and 4b), as is also clear in X-ray maps (Fig. 8). However, the distribution patterns of the particles in the turbid, microperthitic part are not regular in BSE images. Typical X-ray maps of Ca, K, F, and Fe in both the clear and turbid parts are shown in Figures 8 and Figures 9, respectively. It is evident from the two figures that there is a distinct difference of distribution patterns of fluorite particles between both parts of the feldspar crystals. Fluorite particles are randomly distributed in the turbid, microperthitic part (Fig. 9). In addition, it is noted that, for a given area, the number of the particles in the turbid, microperthitic part is slightly less than that in the clear part (Fig. 8 and Fig. 9).

Calcium also is concentrated in other small spots that differ from the positions of fluorite. Randomly distributed Fe-bearing spots are also evident here and there in the turbid and microperthitic part, but they are observed only rarely in the clear part. The positions of the Fe- and Ca-rich spots differ from each other in many cases, and also from the positions of the micropores in general. The nature of these spots has not been ascertained yet, as was the case with Walker et al. (1995), who reported many elements in micropores in feldspars from various syenites and granites. The present TEM observations have revealed only the presence of pyrrhotite flakes.

DISCUSSION

The cooling history of the present alkali feldspar is outlined as follows. The alkali feldspar that crystallized from the magma was around $Or_{40}Ab_{59}An_1$ in bulk-chemical composition. It became cryptoperthitic by exsolution under subsolidus conditions. The cryptoperthite then coarsened during subsequent cooling, and microperthite eventually formed at the hydrother-

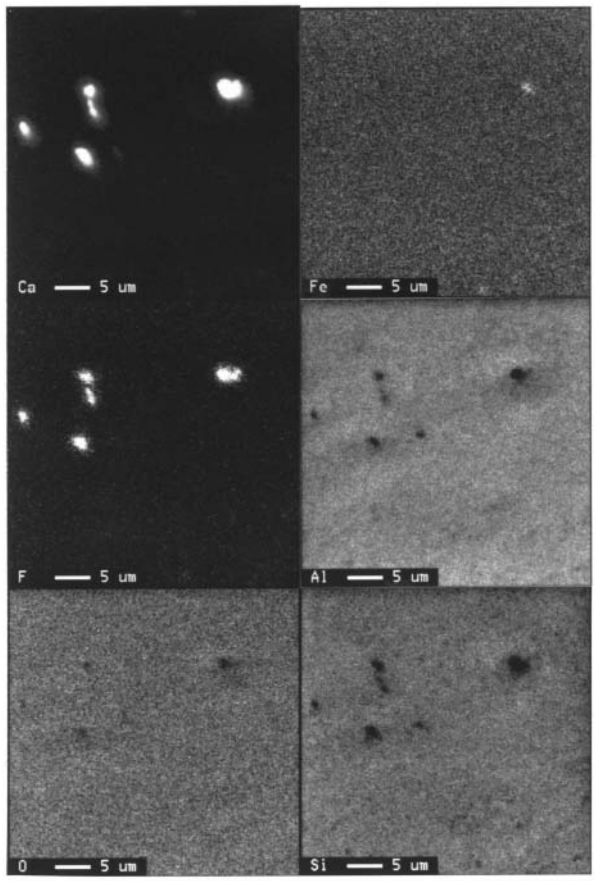

FIGURE 6. X-ray maps of six elements in particles from the centers of butterfly aggregates. The mapping area corresponds to that of the photograph in Figure 3c, although their orientations are at right angles to it.

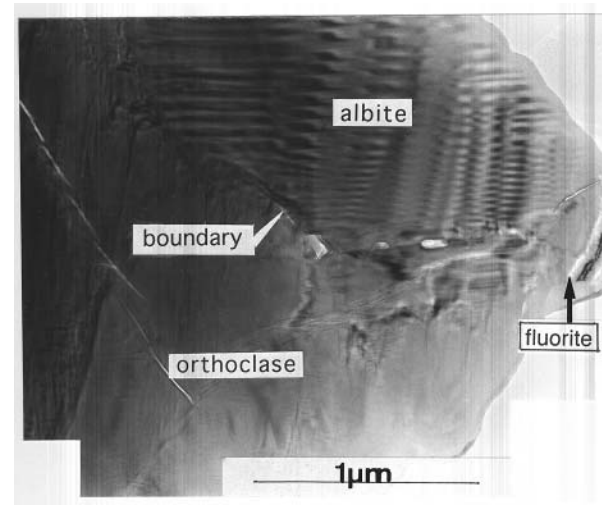

FIGURE 7. TEM photomicrograph of a fluorite particle (at right) enclosed by an Or-rich feldspar (tweed orthoclase, lower half) and an Ab-rich feldspar (albite-twinned albite, upper half).

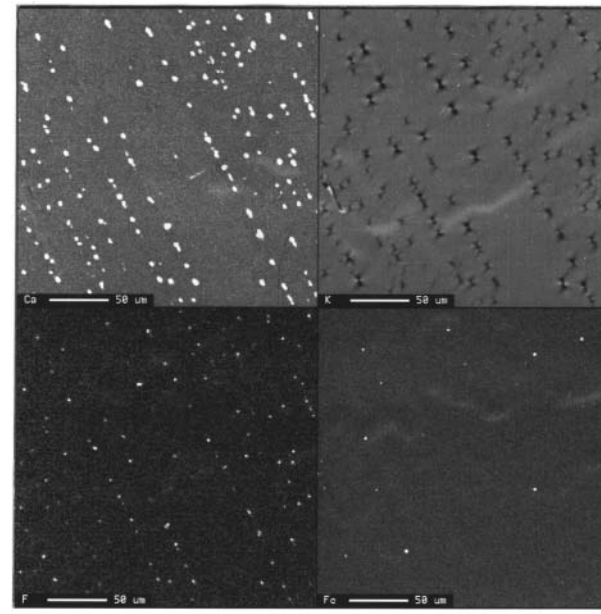

FIGURE 8. X-ray maps of Ca, K, F, and Fe in a clear area containing regularly aligned butterfly aggregates. The mapped area is part of the feldspar grain shown in Figure 2 (lower middle).

mal stage. The butterfly aggregates record an incipient stage of microperthite formation. They changed to patch microperthite with further coarsening. The microperthite is characterized by abundant micropores, as noted in other occurrences (Worden et al. 1990; Brown and Parsons 1994; Walker et al. 1995). The formation of patch microperthite may have been catalyzed by a hydrothermal solution, and thus solution-redeposition may have greatly contributed to its formation (Waldron et al. 1993). Outward transfer of Ca from the feldspar may have occurred during these hydrothermal reactions (Table 1) (Nakano and Akai, in preparation), as was the case of the alkali feldspars from the Japanese syenites reported already (Nakano et al. 1997; Nakano 1998), which induced the present bulk-chemical compositions ($Or_{40}Ab_{59}An_{0.5}$) mentioned already. However, the process and timing of fluorite formation relative to the formation of feldspar textures are uncertain, as discussed below.

The characteristic linear alignment of the fluorite particles in the clear part of the feldspars (Figs. 2, 4, and 8) may be interpreted as either magmatic or subsolidus in origin. The lack of zoning in the distribution of the particles seems to support the latter, and their heterogeneous distributions (and local absence) may also be consistent with the latter. Fluorine is one of the important volatile components in late-stage granitic systems, but fluorite has not been recognized among the primary igneous minerals in such systems (Deer et al. 1963; Kovalenko 1984; London 1987, 1992; Černý 1994). Therefore, the round shape of the fluorite particles (Figs. 4 and 5) may be interpreted to be due not to magmatic corrosion and trapping by feldspar but due to an in-situ growth in feldspar.

Perthitic segregation, or perthite coarsening, along contacts with other minerals or along microcracks or cleavages in alkali feldspars is well known; for example, along contacts with

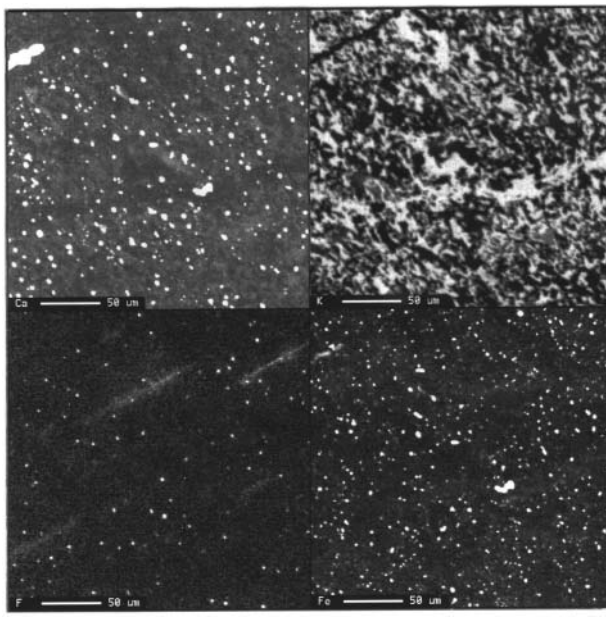

FIGURE 9. X-ray maps of Ca, K, F, and Fe in a turbid and microperthitic area. The mapped area is part of the feldspar grain shown in Figure 1.

subgraphic quartz (Černý et. al. 1984), with deuteric flakes of mica (Černý 1994), and along boundaries with ferromagnesian minerals, subgrain boundaries and cleavages (Lee et al. 1997). The following interpretation, therefore, may be possible concerning the timing of the formation of the fluorite particles. The alkali feldspar developed cryptoperthitic exsolution on cooling of the syenite. An externally derived, F-bearing fluid (or solution) acting as a fluxing component may have introduced microcrystals of fluorite along planes of structural and mechanical weakness in the feldspar, which occurred before microperthite formation. The conversion of cryptoperthite to microperthite, via the butterfly aggregate of incipient microperthite, may have accompanied the growth of the fluorite microcrystals. The butterfly shaped segregation of perthite, or perthite coarsening, could have been promoted either by the presence of an open feldspar surface on contact with fluorite, or by the stress of the growing fluorite. The round shape of fluorite may be due to strain-controlled growth in the feldspar.

Another interpretation concerning the origin of the fluorite warrants some discussion. It is possible that a trace amount of F may occupy some sites in the feldspar structure, although direct evidence for such a substitution has not been obtained. Kovalenko (1984) mentioned this possibility on the basis of numerous F analyses of phenocrysts (including feldspars), groundmass, and whole-rocks. Snow and Kidman (1991) also mentioned the possibility of F incorporation in feldspars based on the results of alkali interdiffusion experiments under low F fugacity. Liu and Nekvasil (2001) suggested the presence of F-bearing, four- and fivefold-coordinated Al species, such as $AlF_3(SiH_3)^-$, in F-bearing alkali aluminosilicate glasses that are precursors of the feldspar structure. Thus, it can be hypothesized that such structural F may have exsolved with Ca, aided by water, to form fluorite in the feldspar.

The difference in the distribution patterns of the fluorite particles in the clear (regular) and turbid parts (irregular) of the feldspar crystals may be interpreted as follows. During hydrothermal reactions that produced the microperthite, the primary, linear alignment of fluorite particles in the pristine cryptoperthitic part was modified to the present irregular distribution patterns through a mechanism of dissolution and reformation. This interpretation is consistent with the fact that the number of fluorite particles in the turbid part is slightly less than in the clear part, as seen in Figures 8 and 9. Solution-redeposition could have caused not only relatively larger-scale transfer of relevant elements during the formation of the patch microperthite but also the above microscopic-scale movement of fluorite particles from the primary positions. Together with these reactions, the hydrothermal event also resulted in the striking concentration of Fe and less so Ca in the patch microperthitic part, although the chemical states or mineral phases associated with these elements are not well identified, except for pyrrhotite.

It is well known that F strongly affects the density and viscosity of silicate melts, fluid-melt partition coefficients of trace elements, mineral-melt equilibria, and cation diffusion rate in melts, as Liu and Nekvasil (2001) summarized, and that F is an important fluxing component in pegmatite environments (London 1992; Černý 1994). In addition, F can have an important role in the textural evolution of alkali feldspars, as noted by Snow and Kidman (1991). The occurrence of fluorite in feldspar has been reported only rarely up to date. Pivec (1974) reported a pseudographic texture of fluorite within alkali feldspar, and attributed its origin to hydrothermal replacement of feldspar by fluorite. As mentioned above, it has been known that F is one of the important components in pegmatites produced from volatile-rich granitic magmas (London 1987, 1992; Černý 1994) and that fluorite occurs in association with feldspar in environments such as pegmatites and hydrothermal deposits (Deer et al. 1966). Only one occurrence of "early formed" fluorite in feldspar has been reported previously. in hypersolvus and related granites from Corsica by Bonin (1984). He demonstrated that epitaxial crystallization of albite occurred on the already formed microcline and on inclusions of (octahedral) fluorite. The present study discusses a different type of occurrence of fluorite in feldspar, and provides new insights into the genetic relation of fluorite and feldspar, and on the behavior of F in alkaline igneous rocks.

ACKNOWLEDGMENTS

The present sample was taken in 1993 during the stay of one of the authors (S. Nakano) in Conception University, Chile, for the project by the Japan International Cooperation Agency. Our sincere thanks are given to the staffs of that university. We are also very grateful to T. Sawaki (Geological Survey of Japan) for his valuable suggestions, B. Roser (Shimane University) for his linguistic review, and P. Černý (University of Manitoba), M.R. Lee (University of Glasgow), and R.F. Martin (McGill University) for their careful and critical reviews that contributed greatly to the revision of the manuscript. In addition, we are also grateful to D. London and R.F. Dymek for careful editorial reviews at the final stage of the revision of the manuscript.

REFERENCES CITED

Bence, R.A. and Albee, A.L. (1968) Empirical correction factors for the electron microanalysis of silicates and oxides. Journal of Geology, 76, 382–403.

Bonin, B. (1986) Ring complex granites and anorogenic magmatism (English translation). 189 p. North Oxford Academic Publishers, London.

Brown, W.L. and Parsons, I. (1988) Zoned ternary feldspars in the Klokken intrusion: exsolution microtextures and mechanisms. Contributions to Mineralogy and Petrology, 98, 444–454.

———(1994) Feldspars in igneous rocks. In I. Parsons, Ed., Feldspars and their reactions, p. 449–499. NATO ASI Ser. C421, Kluwer Academic Publishing, Amsterdam.

Brown, W.L., Lee, M.R., and Parsons, I. (1997) Strain-driven disordering of low microcline to low sanidine during partial phase separation in microperthites. Contributions to Mineralogy and Petrology, 127, 305–313.

Cande, S.C. and Leslie, R.B. (1986) Late Cenozoic tectonics of the southern Chile Trench. Journal of Geophysical Research, 91, 471–496.

Černý, P. (1994) Evolution of feldspars in granitic pegmatites. In W.L. Brown, Ed., Feldspars and feldspathoids, p. 501–540. NATO ASI Series C137, D. Reidel Publishing Company.

Černý, P., Smith, J.V., Mason, R.A., and Delaney, J.S. (1984) Geochemistry and petrology of feldspar crystallization in the VENNA pegmatite, Czechoslovakia. Canadian Mineralogist, 22, 631–651.

Deer, W.A., Howie, R.A., and Zussman, J. (1962) Rock forming minerals, vol. 5. Non-silicates. 371 p. Longmans, London.

Kovalenko, V.I., Antipin, V.S., Kovalenko, N.I., Ryabchikov, I.D., and Petrov, L.L. (1984) Fluorine distribution coefficients in magmatic rocks.

Lalonde, A.E. and Martin, R.F. (1983) The Baie-des-Moutons syenitic complex, La Tabatiere, Quebec, I. Petrography and feldspar mineralogy. Canadian Mineralogist, 21, 65–79.

Lee, M.R., Waldron, K.A., Parsons, I., and Brown, W.L. (1997) Feldspar-fluid interactions in braid microperthite: pleated rims and vein microperthites. Contributions to Mineralogy and Petrology, 127, 291–304.

Liu, Y. and Nekvasil, H. (2001) Ab initio studies of possible fluorine-bearing four- and fivefold coordinated Al species in aluminosilicates glasses. American Mineralogist, 86, 491–497.

London, D. (1987) Internal differentiation of rare-earth element pegmatites: effects of boron, phosphorus, and fluorine. Geochimica Cosmochimica Acta, 51, 403–420.

———(1992) The application of experimental petrology to the genesis and crystallization of granite pegmatites. Canadian Mineralogist, 30, 499–540.

Michael, P.J. (1985) Chemical differentiation of the Cordillera Paine granite (southern Chile) by in situ fractional crystallization. Contributions to Mineralogy and Petrology, 83, 179–195.

———(1991) Intrusion of basaltic magma into a crystallizing granite magma chamber: The Cordillera del Paine Pluton in southern Chile. Contributions to Mineralogy and Petrology, 108, 396–418.

Nakano, S. (1992) Internal textures and chemical compositions of anti-rapakivi mantled feldspars in alkaline igneous rocks from Oki-Dogo island, Japan. Mineralogy and Petrology, 46, 123–135.

———(1998) Calcium distribution patterns in alkali feldspar in a quartz syenite from Oki-Dozen, southwest Japan. Mineralogy and Petrology, 63, 35–48.

Nakano, S., Hosokawa, E., and Akai, J. (1997) Calcium distribution in alkali feldspar of a quartz syenite from Cape Ashizuri, southwest Japan. Mineralogical Journal, 19, 75–86.

Parsons, I. (1978) Feldspars and cooling plutons. Mineralogical Magazine, 42, 1–17.

Parsons, I. and Brown, W.L. (1984) Feldspars and the thermal history of igneous rocks. In Brown, W.L., Ed., Feldspars and feldspathoids, p. 317–371. NATO ASI Series C137, D. Reidel Publishing Company, Dordrecht, Holland.

Piveč, E. (1974) Pseudographic potash feldspar-fluorite intergrowths from Krupka near Teplice-spa (Krusné Hory Mts), Czechoslovakia. Neues Jahrbuch für Mineralogie Monatshefte, H.10, 447–453.

Smith, J.V. and Brown, W.L. (1988) Feldspar minerals, 828p. Springer, Berlin.

Snow, E. and Kidman, S. (1991) Effect of fluorine on solid-state alkali interdiffusion rates in feldspar. Nature, 349, 17 January, 231–233.

Waldron, K. and Parsons, I. (1992) Feldspar microtextures and multistage thermal history of syenites from the Coldwell Complex, Ontario. Contributions to Mineralogy and Petrology, 111, 222–234.

Waldron, K., Parsons, I., and Brown, W.L. (1993) Solution-redeposition and the orthoclase-microcline transformation: evidence from granulites and relevance to ^{18}O exchange. Mineralogical Magazine, 57, 687–695.

Walker, F.D.L., Lee, M.R., and Parsons, I. (1995) Micropores and micropermeable texture in alkali feldspars: geochemical and geophysical implications. Mineralogical Magazine, 59, 505–534.

Worden, R., Walker, F.D.L., Parsons, I., and Brown, W.L. (1990) Development of microporosity, diffusion channels and deuteric coarsening in perthitic alkali feldspars. Contributions to Mineralogy and Petrology, 104, 507–514.

MANUSCRIPT RECEIVED JUNE 7, 2001
MANUSCRIPT ACCEPTED APRIL 24, 2002
MANUSCRIPT HANDLED BY DAVID LONDON

APPENDIX: ANALYTICAL METHODS

Textural observations were made at Shiga University with an optical microscope and by back-scattered electron images (BSE) and secondary electron images (SEI) with an electron probe microanalyzer (EPMA: JEOL JXA 8800M). Quantitative analyses and X-ray mapping were also undertaken using the same EPMA. The operating conditions were 15 kV accelerating voltage, 0.02 μA probe current, focused beam for image observations, and either 5 or 50 μm beam for quantitative analyses. Quantitative analyses were made according to the Bence and Albee (1968) correction method using oxides and silicates as standards, as well as the previous analyses reported already (e.g., Nakano 1992, 1998). Counting times are 10 sec for peak measurements and 5 sec for background measurements. Mapping was made under the conditions: 15 kV, 0.06 μA, focused beam, 500 × 500 pixels and about 100 μs counting time per one pixel. Transmission electron microscopic (TEM) observations were made with a JEM CX200 electron microscope (JEOL) of Niigata University, operating at 160 kV. EDS analyses with TEM were carried out using a Voyer IV/TN 2000 system produced by Northan Instruments Co. Ltd. Sample preparation for TEM observations was made using an ion beam thinning apparatus, Edwards IBT200.